# Performance of mixed phase $TiO_2$ film samples immobilized on a 2-D flat plate surface in photo catalytic applications and reusability

**Tripurari Kumar Harsh[1, 2,3], S K Samdarshi[1, 2,3*], Uday Deshpande[3] , Bhola Kumar[1], Md. Rahbar Jamal[1,2], Rahul Kumar Rajak[1], and A.S Bhattacharya[2]**

[1] Department of Energy Engineering, Central University of Jharkhand, Ranchi (India)

[2] Centre of Excellence in Green and Efficient Energy Technology, CUJ, Ranchi, Jharkhand (India)

[3] UGC-DAE CSR, Indore 452001,MP (India)

## Abstract

$TiO_2$ is well known photocatalyst for environmental remediation technology with a green approach of oxidation and reduction using solar irradiation. In this study three $TiO_2$ samples were successfully synthesized using sol-gel method and then calcined at 550°C, 650°C and 750°C(termed as Ti-550, Ti-650, and Ti-750, respectively). The prepared nano-powder samples were immobilized as two dimension (2-D) thin film over glass plate surface using doctor-blade method. The characterization of the prepared photocatalysts was done using X-Ray diffractometer (XRD), UV-Vis diffuse reflectance spectroscopy (DRS) and photoluminescence (PL) spectroscopy. The resultant samples were nanoscale systems of pure anatase, and anatase-rutile mixed phase. The band gap of the nano-catalyst samples Ti-550, Ti-650, and Ti-750 were found to be 3.04 eV, 2.97 eV, and 2.92 eV, respectively. The theoretical modeling and analysis of the samples was done by Materials Studio® software and the optical characterization was done with its CASTEP module using DFT. The performance of the samples was studied by methylene blue (MB) dye degradation kinetics under solar radiation (avg. 955 W/m$^2$) outdoors. We conducted reusability tests on the coated samples for three cycles, with the Ti-650 sample exhibiting the highest rate constant in each degradation cycle. This may be attributed to the suitable band gap, phase ratio, and the resultant reduction in recombination of the photo-generated charge-carriers of the nano-samples. The rate constants of three continuous cycle of Ti-650 thin flim samples were calculated to be 0.00809, 0.00511 and 0.00508 per minute wherein a stabilization in performance is seen after second cycle.

*Keywords: Titania, Mixed phase, Thin flim, Phase ratio, Reusability, Theoretical analysis*

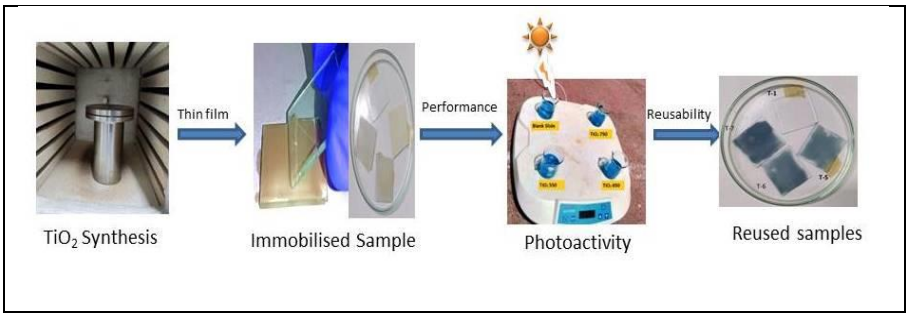


## 1. Introduction

As energy and environmental concerns and the need for sustainable solutions continue to grow, the utilization of titanium dioxide ($TiO_2$) thin films for the degradation of organic pollutants under outdoor solar irradiation has emerged as a promising and eco-friendly approach. $TiO_2$ thin films have garnered significant attention due to their abundance, exceptional photocatalytic properties, durability, and reusability, making them a valuable and versatile semiconductor material with a wide range of applications in various fields of photocatalytic hydrogen production, carbon valorization, including environment remediation [1-3].

$TiO_2$ exists in several crystalline phases, with the three most common ones being anatase, rutile, and brookite


Selection and/or peer review under responsibility of Scientific Committee
10.18086/swc.2023.13.01 Available at http://proceedings.ises.org

phase. Each of these phases possesses distinct structural and electronic characteristics that influence their catalytic performance under solar irradiation. The bandgap of anatase and brookite $TiO_2$ falls within the ultraviolet (UV) region of the electromagnetic spectrum, and are highly effective in utilizing UV solar radiation for photocatalytic reactions. Anatase $TiO_2$ has been extensively employed in applications such as water splitting, pollutant degradation, and hydrogen production due to its exceptional photoactivity. The rutile phase of $TiO_2$ is another important crystalline form, known for its exceptional stability and relatively narrower bandgap compared to anatase. Rutile $TiO_2$ is less active under UV light but becomes increasingly efficient under visible light irradiation. The mixed phase of $TiO_2$ is the least common among the three major phases but is gaining attention for its unique photocatalytic properties. Understanding the unique properties and capabilities of each of the $TiO_2$ phase is essential for harnessing their full potential in sustainable and energy-efficient photocatalytic processes, contributing to a cleaner and more sustainable future [3-14].

The utilization of titanium dioxide ($TiO_2$) immobilized onto a substrate in the form of thin films has emerged as a promising and eco-friendly approach due to their exceptional durability, reusability, and insignificant loss of the catalyst, making it a valuable system. $TiO_2$ thin films are engineered structures that consist of a thin layer of $TiO_2$ deposited onto a multidimensional substrate. These films possess several advantages for photocatalytic applications under outdoor conditions. Furthermore, the thin film format allows for easy integration into various outdoor settings, for some specific applications such as wastewater treatment plants, polluted air purification systems, and self-cleaning surfaces on buildings and infrastructure including others [15-21].

As indicated, one of the most remarkable features of $TiO_2$ thin films is their reusability. Unlike some traditional catalysts that degrade or require regeneration after a single use, $TiO_2$ thin films can be employed repeatedly without significant loss of catalyst material and catalytic activity. This property is of utmost importance for cost-effectiveness and sustainability. By simply exposing the thin films to natural outdoor sunlight, any absorbed/adsorbed organic pollutants or other reactive species are degraded, and the catalyst is regenerated, and is ready for reuse. The reusability of $TiO_2$ thin films not only reduces operational costs but also minimizes the environmental footprint of pollution remediation and energy conversion processes. This approach aligns with the principles of green chemistry and sustainable development, contributing to a cleaner and healthier environment. Moreover, the ability to deploy these thin films in outdoor settings means that they can address pollution at its source, preventing the accumulation of harmful substances in our ecosystems [22, 23].

## 2. Experimental details

### 2.1. Synthesis of nanoparticles

The synthesis of mixed phase $TiO_2$ nanoparticles using the sol gel method of synthesis of titanium dioxide is a well-known technique. Titanium tetra isopropoxide (TTIP) was purchased from Sigma-Aldrich, and isopropyl alcohol from Merck, India. The triton X solvent (LR grade) was from Sigma-Aldrich, India. In all of the experiments, double-distilled water was used, and all of the chemicals employed in the synthesis were of analytical grade. TTIP and 2-propanol were taken in 1:10 ratio. After 15 minutes, 0.5 mL of DI water was added in the sol while being constantly stirred for 16 hours. The produced gel was aged for 12 hours and then dried at 80$^{o}$C for 12 hours. To obtain crystalline nanoparticles, the final product was calcined in air for two hours at 550, 650, and 750$^{o}$C with a ramping rate of 5$^{o}$C. Henceforth, these samples are referred to as Ti-550 , Ti-650 and Ti-750 respectively.

### 2.2. Characterization

The structural properties of titanium dioxide samples prepared at different temperatures were analyzed by X-ray diffractometer (Proto AXRD Benchtop, Canada). The spectral response was assessed using UV–Vis–NIR spectrophotometer with DRS (UV 3600 Plus, Shimadzu, Japan). The trap states of the samples were identified using photoluminescence (PL) spectrum obtained from photoluminescence spectrometer (Fluromax-4, Horiba Scientific, USA).

### 2.3 Thin film deposition

The glass substrate we thoroughly cleaned using acetone, water, and sonication; and then dried. The photocatalyst material was formed into slurry for this to create the binder solution; the photocatalyst nano particles (20 mg), triton X solvent (2 drops), and acetic acid (2 drops) were progressively mixed. Using the doctor blade approach, the photocatalyst slurry of was applied to the substrate surface. After deposition, the layer was kept at 60°C on a hot plate for two hours before cooling in the open to form a stable film on the substrate [Fig.1].

### 2.4 Photocatalytic activity test:

The activity of the immobilized catalyst was evaluated by the degradation kinetics of aqueous methylene blue as probe pollutant over it under outdoor solar irradiation. The degradation kinetics was assessed under a catalyst loading of 0.5 g/l. To ensure adsorption-desorption equilibrium the system was initially kept in dark for 30 min. Then, the system was exposed to outdoor solar irradiation and sampling was done at an interval of 30 min. Finally, the collected sample was centrifuged before conducting photometric studies on the resultant solution for degradation analysis.

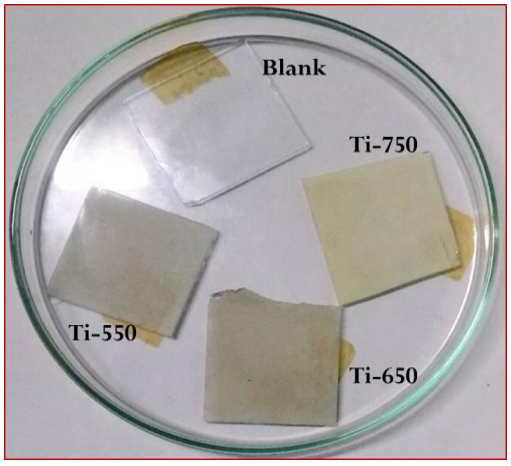


**Fig.1: Different $TiO_2$ samples coated on plate surface**

## 3. Result & discussion:

### 3.1. XRD analysis

Fig.2 shows the XRD spectra of $TiO_2$ nanoparticles samples. From XRD pattern it is revealed that the Ti-550 corresponds to pure anatase phase (JCPDS File No.894203). The samples Ti-650 and Ti-750 both correspond to anatase-rutile mixed phase (JCPDS File No.894203 and 894920). The crystallite sizes of the particles were calculated using Scherrer's formula, $D=k\lambda/\beta\cos\theta$; where D is the average crystallite size and k is the shape factor taken as 0.9, λ is the wavelength of X-ray radiation (Cu Kα =1.5406 Å), β is the full width at half-maximum intensity (in radian) and θ is the diffraction angle. The anatase and rutile mass fraction and anatase to rutile (A/R) ratio were calculated using Spurr's equation: $fa= (1+1.26Ir/Ia)^{-1}$, fr= (1-fa) and A/R= (fa/fr); where fa and fr are anatase and rutile mass fraction, and Ia and Ir are the most intense anatase and rutile peak, respectively [9-11]. The crystallite size and phase composition of each $TiO_2$ nanoparticles at different temperatures are given in Table.1. XRD spectra reveal that at temperature 550$^o$C pure anatase phase was formed. The mixed phase transition was identified at 650$^o$C which could be seen to continue up to 750$^o$C in the form of anatase and rutile. The crystallite size as well as rutile ratio of the samples increased with the increase in the temperature.

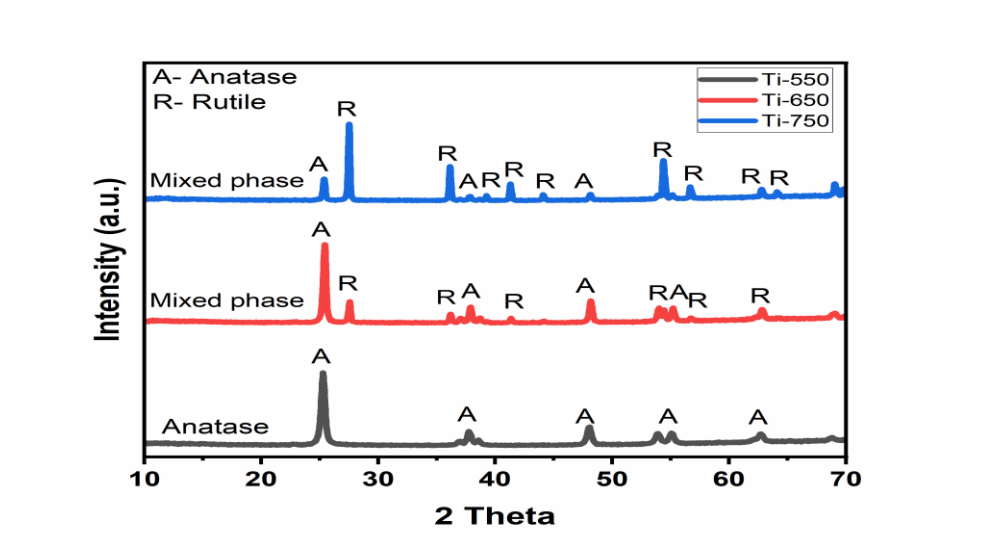


**Fig.2. XRD pattern of titanium dioxide catalyst calcined at different temperatures**

**Tab 1: Shows the crystallite size and phase composition of $TiO_2$ nanoparticles at different temperatures**

| Sample | Calcination temp ($^oC$) | Crystallite size (nm) | | Fraction (%) | | A/R ratio |
|---|---|---|---|---|---|---|
| | | Anatase (A) | Rutile (R) | Anatase | Rutile | |
| Ti-550 | 550 | 20.56 | 0 | 100 | 0 | ∞ |
| Ti-650 | 650 | 28.18 | 36.29 | 72.82 | 27.18 | 2.68 |
| Ti-750 | 750 | 35.40 | 40.22 | 19.47 | 80.53 | 0.24 |

## 3.2. UV-VIS DRS analysis

The optical characteristics of the samples were examined using the UV-VIS DRS spectra. In Fig. 3(a) and (b), samples that were calcined at a higher temperature exhibit a red shift in the wavelength. As the calcination temperature rises, the samples band gap gradually narrows. Absorbance was obtained from the diffuse reflectance using Kubelka-Munk transformation. Bandgap was calculated from the Kubelka-Munk absorbance using Tauc plot shown in Fig. 3(b). The band gap variations between the samples can be attributed to thermally induced defects in the red-shifted samples and changes in the crystallite phases of the individual samples. It is evident from the bandgap (i.e. 2.9eV-3.1 eV) that the samples absorb in UV-Vis range of solar spectrum so it would be interesting to study the photoactivity in the outdoor solar spectra.

(a) (b)

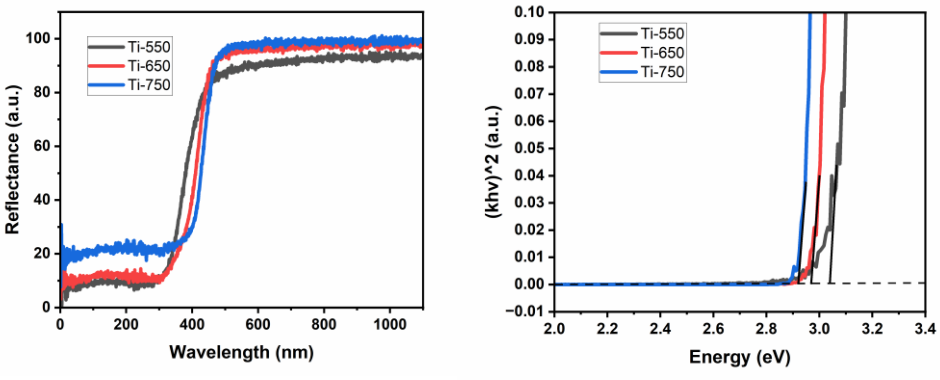


**Fig.3: (a) UV–Vis diffuse reflectance spectra of samples (b) Bandgap of the prepared samples**

## 3.3. PL spectra analysis

The photoluminescence spectra of the samples were recorded at the six different excitation wavelengths starting from 325 nm to 425 nm in the progressive interval of 25 nm and at 500 nm. Fig 3(a) shows that at high energy photon excitation the rutile dominant mixed phase has high quenching and hence least carrier recombination. Fig 3(b) also has similar results but, in this case, the emission wavelength peaks at the lower wavelengths 405 nm, 440 nm and 450 nm correspond to the band gap of the Ti-550, Ti-650 and Ti-750 samples, respectively, which may be attributed to the close proximity of the excitation wavelength to the band gap.. Figs 3(c) and (d) provide identical conclusion with poor resolution attributable to the excitation wavelength. Interestingly, with excitation wavelength in or close to visible range the quenching pattern shows a reversal with Ti-750 (mixed phase) showing least quenching with high intensity emission and, hence, high recombination (Fig 3(e) and (f)). Thus, the low temperature samples are expected to show more photocatalytic activity. But high quenching in Ti-550 may be because of low emission due to decreased absorption of low energy excitation wavelength. Ti-650, however, shows genuine non-zero quenching attributatble to decreased recombination. Ti-750 shows high quenching in spite of high conductivity which may because resonance of the excitation wavelength with the system trap level/band gap as shown in fig (a-d). The broad peaks between 400 nm to 650 nm may be attributed to the presence of the defects state and oxygen vacancies at higher temperature. It is evident from the PL spectra that recombination in the sample treated at higher temperature is lowered as compared to the samples treated at lower temperatures, This may be due to higher oxygen vacancies created in the high temperature samples due to induced defect levels and change in the crystallite phases.

(a) (b) (c)

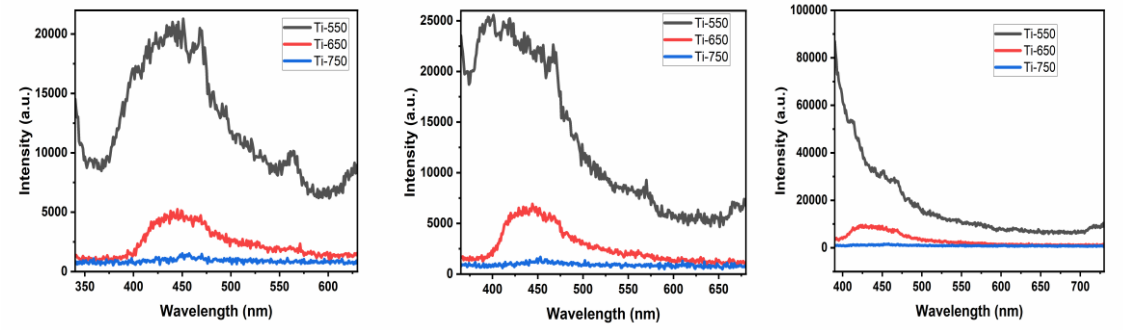

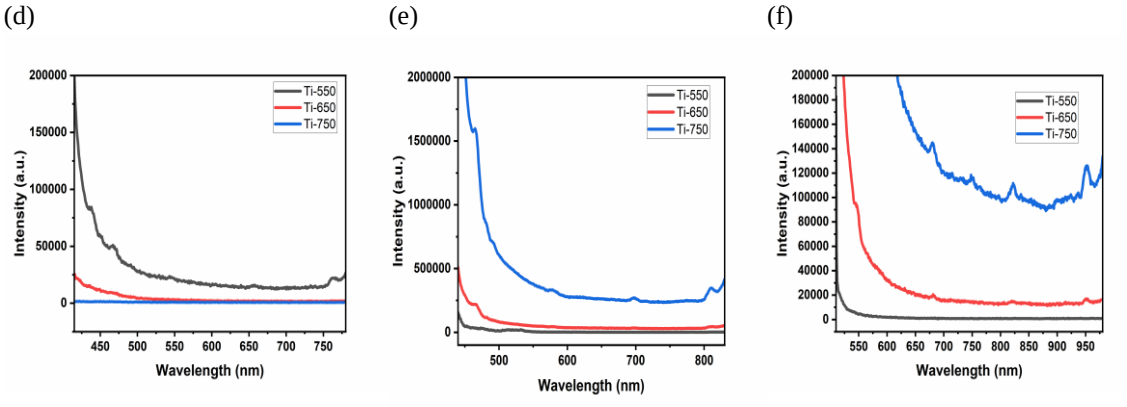


**Fig. 4: Photoluminescence excitation spectra of samples at high energy (UV) wavelength of (a) 325nm (b) 350nm (c) 375 nm (d) 400nm and at low energy (Visible) wavelength of (e) 425 nm and (f) 500nm.**

## 3.4. Computational modeling and analysis:

This theoretical analysis has been conducted using the Perdew-Burke-Ernzerhof module programme in BIOVIA Materials Studio version 2017 R2 (Dassault Systems). It was combined with an ultra-soft pseudo potential and a plane wave basis set with a kinetic energy cut-off of 380 eV. For the theoretical investigation, the anatase and rutile phases of the titanium crystal structure were used. Electronic band structures of the crystals were calculated using Koelling-Harmon grid settings on the optimized geometry crystal with 3×3×2 k-points sampling. Atomic coordinates and cell parameters were optimized during the iterative optimization process. The CASTEP computation calculation and analysis were performed on the optimized crystal band. The band gap of a anatase structure was larger than a rutile structure. The band gap ($E_g$) and density of states (DOS) of anatase(101) and rutile(110) phase layer were 2.078, and 1.879eV respectively as shown in the fig.5 its prediction is always less than the experimental analysis and supports the order of the bandgap of phases of the samples [24,25].

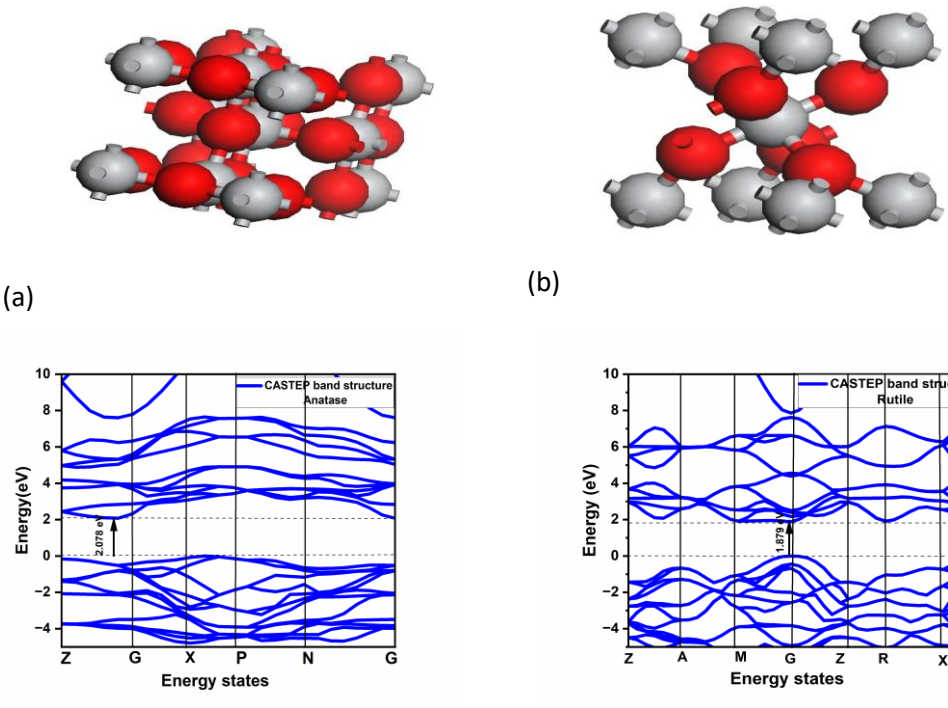

**(c)**

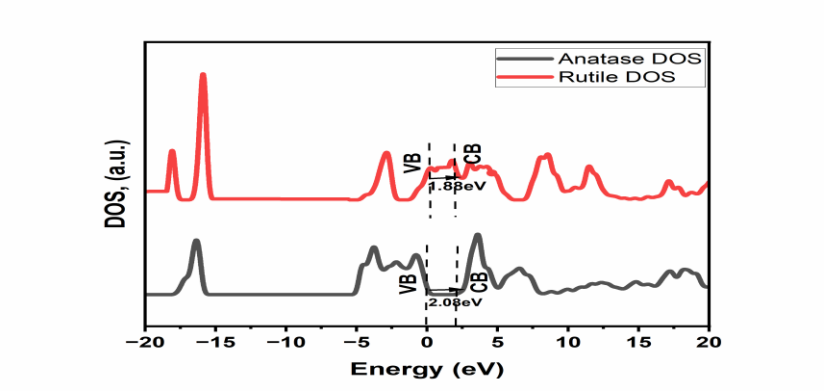


**Fig.5: Crystal structure and bandgap of (a) anatase and (b) rutile, respectively; Crystal (Note: Red and white sphere represent oxygen and titanium, respectively (c) Density of states of anatase and rutile**

## 4. Photo-activity analysis

The photoactivity test of the photocatalyst was performed under available outdoor solar irradiation during solar noon (900-970 W/m$^2$, Table 2) using methylene blue dye degradation. The dye degradation rate of each sample is calculated using pseudo-first order kinetics. The calculated band gap and rate constant is given in the Table 3 The rate constant value discloses that the mixed phase samples are more active in outdoor solar irradiation. The kinetics of degradation of rate constant of reusability activity of three cycles is shown in fig.6. The photocatalytic rate constant for Ti-650 sample is the highest in each cycle. The catalyst weight loss after each cycle activity is shown in the table 4. The catalyst weight loss is more in the first cycle activity and then becomes stable and very less catalyst loss of each sample afterwards cycle. This may be as a result of the creation of higher oxygen vacancies induced trap states as well as band offset at the rutile-anatase interface.

**Tab 2: Outdoor solar radiation data**

| **Activity time** | 10:30 am | 11:00 am | 11:30 am | 12:00 pm | 12:30 pm | 01:00 pm |
|---|---|---|---|---|---|---|
| **Direct Solar Irradiation(W/m$^2$)** | Dark | 955 | 970 | 965 | 970 | 900 |

**Tab. 3: Calcined temperature, Band gap and rate constant in outdoor irradiation for different samples.**

| Sample | Calcined temperature($^o$C) | Bandgap (eV) | Rate constant (K) in outdoor solar irradiation (min$^{-1}$) | | |
|---|---|---|---|---|---|
| | | | Test 1 | Test 2 | Test 3 |
| Blank | -- | -- | 0.00349 | 0.00336 | 0.00359 |
| Ti-550 | 550 | 3.04 | 0.00636 | 0.00425 | 0.00400 |
| Ti-650 | 650 | 2.97 | 0.00809 | 0.00511 | 0.00508 |
| Ti-750 | 750 | 2.92 | 0.00723 | 0.00453 | 0.00418 |

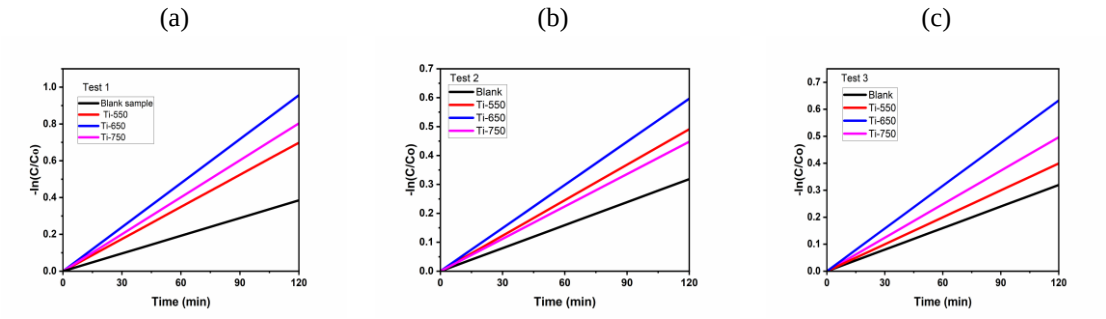


**Fig.6: Kinetics of degradation for calculation of rate constant of reusability activity (a) cycle test 1 (b) cycle test 2 and (c) cycle test 3.**

**Tab:4 Catalyst weight loss after each cycle of degradation activity**

| Sample | Blank slide weight (mg) | Coated weight (mg) | Weight after reusability (mg) | Weight after second reusability(mg) | Weight after third reusability(mg) |
|---|---|---|---|---|---|
| Blank slide | 2144.80 | 2144.80 | 2144.80 | 2144.80 | 2144.80 |
| Ti- 550 | 2149.77 | 2163.10 | 2159.05 | 2157.70 | 2757.05 |
| Ti- 650 | 2179.12 | 2192.82 | 2189.40 | 2187.62 | 2187.25 |
| Ti- 750 | 2064.05 | 2077.42 | 2074.00 | 2072.21 | 2071.77 |

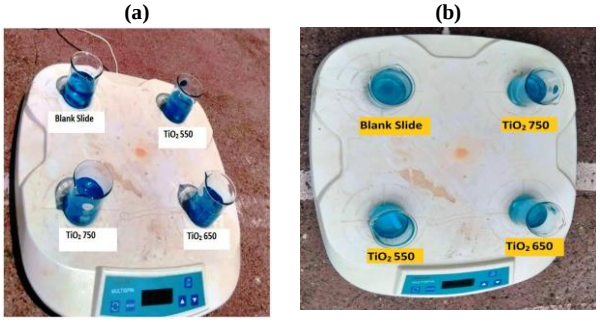


.

**Fig.7: photoactivity test (a) before and (b) after**

## 5. Mechanism

The high photo activity under outdoor solar irradiation may be ascribed to the interfacial behavior of the band offset and oxygen vacancies in mixed phase titania nanoparticles. The band gap and carrier recombination are both significantly reduced when there are defects at the junction, which raises the photocatalytic activity. The mechanism shown in Fig 9(a) and (b) has been framed based on the behavior of PL spectra of the samples at different excitation wavelength, wherein, there is a reversal of quenching after an excitation wavelength of 400nm, i.e in the visible range [9]. The movement of the carriers under UV and visible irradiation, respectively, are shown in Fig 9(a) and 9(b).

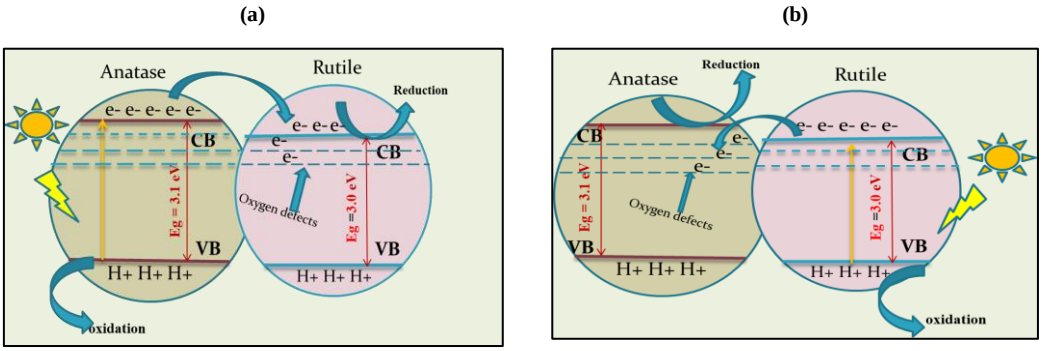


**Fig.9: highly active mixed phase junction of anatase and rutile for (a) wavelength < 400nm (b) wavelength > 400nm.**

## 6. Conclusion

$TiO_2$ thin films represent a remarkable and sustainable solution for the degradation of organic pollutants under outdoor solar irradiation. Mixed phase Ti-650 samples shows highest rate constant which may be attributed to their suitable bandgap, anatase-rutile phase ratio, defect states, band offset and the crystallite size. The ability of mixed phase thin films to harness solar radiation, together with their reusability, places them as a vital technology in the quest for environmental remediation and other energy applications.. The reusable application of $TiO_2$ thin films holds great promise for a more sustainable and cleaner future.

## 7. Acknowledgments

1) This work was carried out using the facilities of Centre of Excellence in Green and Efficient Energy Technology (CoE-GEET), DEE, Central University of Jharkhand, Ranchi-835205

2) “This work was partially carried out using the facilities of UGC-DAE CSR. The authors acknowledge the financial support from UGC-DAE CSR through a Collaborative Research Scheme (CRS) project number CRS/2021-22/01/403”

## 8. References

1) Athanasekou, Chrysoula P., Vlassis Likodimos, and Polycarpos Falaras. "Recent developments of TiO2 photocatalysis involving advanced oxidation and reduction reactions in water." Journal of environmental chemical engineering 6.6 (2018): 7386-7394.

2) Wei, Yaqing, Marina V. Tokina, Alexander V. Benderskii, Zhaohui Zhou, Run Long, and Oleg V. Prezhdo. "Quantum dynamics origin of high photocatalytic activity of mixed-phase anatase/rutile $TiO_2$." *The Journal of Chemical Physics* 153, no. 4 (2020).

3) Liu, Hongli, Yaping Ma, Jiangyao Chen, Meicheng Wen, Guiying Li, and Taicheng An. "Highly efficient visible-light-driven photocatalytic degradation of VOCs by $CO_2$-assisted synthesized mesoporous carbon confined mixed-phase $TiO_2$ nanocomposites derived from MOFs." *Applied Catalysis B: Environmental* 250 (2019): 337-346.

4) Lin, Xiaojing, Mingxuan Sun, Bowen Gao, Wen Ding, Zihan Zhang, Sambandam Anandan, and Ahmad Umar. "Hydrothermally regulating phase composition of $TiO_2$ nanocrystals toward high photocatalytic activity." *Journal of Alloys and Compounds* 850 (2021): 156653.

5) Paumo, Hugues Kamdem, Sadou Dalhatou, Lebogang Maureen Katata-Seru, Boniface Pone Kamdem, Jimoh Oladejo Tijani, Venkataraman Vishwanathan, Abdoulaye Kane, and Indra

Bahadur. "$TiO_2$ assisted photocatalysts for degradation of emerging organic pollutants in water and wastewater." *Journal of Molecular Liquids* 331 (2021): 115458.

6) Lal, Manmohan, Praveen Sharma, and Chhotu Ram. "Calcination temperature effect on titanium oxide ($TiO_2$) nanoparticles synthesis." *Optik* 241 (2021): 166934.

7) Kim, Min Gu, Jeong Min Kang, Ji Eun Lee, Kang Seok Kim, Kwang Ho Kim, Min Cho, and Seung Geol Lee. "Effects of calcination temperature on the phase composition, photocatalytic degradation, and virucidal activities of $TiO_2$ nanoparticles." *ACS omega* 6, no. 16 (2021): 10668-10678.

8) Assayehegn, Elias, Ananthakumar Solaiappan, Yonas Chebude, and Esayas Alemayehu. "Fabrication of tunable anatase/rutile heterojunction N/TiO2 nanophotocatalyst for enhanced visible light degradation activity." *Applied Surface Science* 515 (2020): 145966.

9) Verma, Ranjana, and S. K. Samdarshi. "Correlating oxygen vacancies and phase ratio/interface with efficient photocatalytic activity in mixed phase TiO2." *Journal of Alloys and Compounds* 629 (2015): 105-112.

10) Nair, Ranjith G., Samrat Paul, and S. K. Samdarshi. "High UV/visible light activity of mixed phase titania: A generic mechanism." *Solar energy materials and solar cells* 95, no. 7 (2011): 1901-1907.

11) Verma, Ranjana, S. K. Samdarshi, Kalpana Sagar, and B. K. Konwar. "Nanostructured bi-phasic TiO2 nanoparticles grown on reduced graphene oxide with high visible light photocatalytic detoxification." *Materials Chemistry and Physics* 186 (2017): 202-211.

12) Ramchiary, Anjalu, S. K. Samdarshi, and T. Shripathi. "Hydrogenated mixed phase Ag/TiO2 nanoparticle–A super-active photocatalyst under visible radiation with multi-cyclic stability." *Solar Energy Materials and Solar Cells* 155 (2016): 117-127.

13) Ali, Imran, Gi-Beom Han, and Jong-Oh Kim. "Reusability and photocatalytic activity of bismuth-TiO2 nanocomposites for industrial wastewater treatment." *Environmental research* 170 (2019): 222-229.

14) Lin, Xiaojing, Mingxuan Sun, Bowen Gao, Wen Ding, Zihan Zhang, Sambandam Anandan, and Ahmad Umar. "Hydrothermally regulating phase composition of TiO2 nanocrystals toward high photocatalytic activity." *Journal of Alloys and Compounds* 850 (2021): 156653.

15) Samy, Mahmoud, Mona G. Ibrahim, Mohamed Gar Alalm, Manabu Fujii, Shinichi Ookawara, and Teruhisa Ohno. "Photocatalytic degradation of trimethoprim using S-TiO2 and Ru/WO3/ZrO2 immobilized on reusable fixed plates." *Journal of Water Process Engineering* 33 (2020): 101023.

16) Mahmood, Asad, and Jae-Woo Park. "TiO2/CdS nanocomposite stabilized on a magnetic-cored dendrimer for enhanced photocatalytic activity and reusability." *Journal of colloid and interface science* 555 (2019): 801-809.

17) Shen, Yinghua, Xiang Yu, Weitian Lin, Yi Zhu, and Yuanming Zhang. "A facile preparation of immobilized BiOCl nanosheets/TiO2 arrays on FTO with enhanced photocatalytic activity and reusability." *Applied Surface Science* 399 (2017): 67-76.

18) Moma, John, and Jeffrey Baloyi. "Modified titanium dioxide for photocatalytic applications." Photocatalysts-Applications and Attributes 18 (2019): 10-5772.

19) Kocijan, Martina, Lidija Ćurković, Igor Bdikin, Gonzalo Otero-Irurueta, María J. Hortigüela, Gil Gonçalves, Tina Radošević, Damjan Vengust, and Matejka Podlogar. "Immobilised rGO/TiO2 nanocomposite for multi-cycle removal of methylene blue dye from an aqueous medium." Applied Sciences 12, no. 1 (2022): 385.

20) Raza, N., Raza, W., Gul, H., Azam, M., Lee, J., Vikrant, K., & Kim, K. H. (2020). Solar-light-active silver phosphate/titanium dioxide/silica heterostructures for photocatalytic removal of

organic dye. Journal of Cleaner Production, 254, 120031.

21) Ali, I., Han, G.B. and Kim, J.O., 2019. Reusability and photocatalytic activity of bismuth-TiO2 nanocomposites for industrial wastewater treatment. Environmental research, 170, pp.222-229.

22) Bento, Rodrigo T., Olandir V. Correa, and Marina F. Pillis. "On the surface chemistry and the reuse of sulfur-doped TiO2 films as photocatalysts." Materials Chemistry and Physics 261 (2021): 124231.

23) Malakootian, Mohammad, Alireza Nasiri, and Majid Amiri Gharaghani. "Photocatalytic degradation of ciprofloxacin antibiotic by TiO2 nanoparticles immobilized on a glass plate." Chemical Engineering Communications 207, no. 1 (2020): 56-72.

24) Xing, Jiahui, Yuzheng Wang, Yusheng Wu, Laishi Li, and Pengwei Liu. "Influence of calcination temperature on the microstructure and photocatalysis performance of B/Sm-TiO2 nanomaterials." *Vacuum* 212 (2023): 112063.

25) Ibrahim, Qusai, Rokhsareh Akbarzadeh, and Salem Gharbia. "The electronic properties and water desalination performance of a photocatalytic TiO2/MoS2 nanocomposites bilayer membrane: A molecular dynamic simulation." *Journal of Molecular Modeling* 28, no. 3 (2022): 61.